

Enhancing Autoencoder Performance: Leveraging Gain and Relative Gain Array (RGA) Through Innovative Functions for Training Optimization and Pruning

Rafael Henrique Martello^a, Marcelo Farenzena^a, Jorge Otávio Trierweiler^a

^a*Group of Intensification, Modeling, Simulation, Control, and Optimization of Process, GIMSCOP, Federal University of Rio Grande do Sul, Chemical Engineering Department, St. Engenheiro Luiz Englert - 12.204, Porto Alegre, 90040-040, RS, Brazil*

Abstract

High-dimensional data poses significant challenges in modern data science, necessitating innovative approaches for effective processing and extracting meaningful insights. Autoencoders, a type of neural network, offer a promising solution by leveraging the latent space representation to extract valuable information from complex datasets. However, optimizing autoencoders remains challenging due to the high dimensionality, nonlinearity, and potential for overfitting or underfitting. To address these issues, this study introduces two novel objective functions based on the concepts of the Gain Matrix (G) and Relative Gain Array (RGA), along with pruning techniques, to enhance autoencoder training and performance. A case study of a simulated propene production plant is used to demonstrate the effectiveness of the proposed approach. The results reveal that autoencoders with novel objective functions outperform traditional methods, such as PCA and conventional autoencoders with mean square error (MSE) objective functions, leading to gains of up to 40% in the explained variance when compared to a PCA and up to 20% when compared to usual autoencoders. The findings underscore the potential of autoencoders as powerful tools for high-dimensional data analysis. By incorporating multivariable control concepts and refining objective functions, autoencoders offer new opportunities to address complex data challenges and advance data science in diverse real-world scenarios.

Keywords: Unsupervised Learning, Multivariable Control, Data Compression, Soft-Sensors

1. Introduction

High-dimensional data is a pervasive challenge across various domains of modern data science. The curse of dimensionality looms over the analysis of such data, requiring innovative approaches for effective processing and extraction of meaningful insights [1]. In this context, autoencoders emerge as a promising solution, offering a powerful framework to tackle the complexities of high-dimensional data. By leveraging the latent space representation generated by autoencoders, valuable information can be extracted, enabling improved predictions, classifications, and data-driven decision-making [2].

10 Autoencoders are a type of neural network that learns in an unsupervised
11 way, and they were first introduced as a model that is trained to reconstruct
12 its input instead of relying on labeled data. It relies on the relationship
13 between the input variables [3, 4]. They have many applications, including
14 assisting in classifications, regressions, and performing unsupervised tasks in
15 high-dimensional spaces, such as data compression, denoising, dimensionality
16 reduction, and feature extraction [5, 6]. As shown in [3, 7], there are numerous
17 applications of AEs and their variants, focused on sound [8, 9] to image and
18 video data [10, 11].

19 In the realm of data-driven decision-making, soft-sensors have emerged
20 as valuable tools for capturing real-time information from complex systems.
21 These virtual sensors, derived from machine learning techniques, provide a
22 means to extract meaningful and actionable insights from raw data streams
23 [12, 13]. Previous studies have explored soft-sensors based on neural networks
24 [14] using a PCA followed by a supervised adaptive network-based fuzzy
25 inference system (ANFIS) for the prediction of carbon and nitrogen removal
26 in wastewater treatment, [15] a supervised feed-forward artificial neural network
27 to provide estimates of the polyethylene terephthalate (PET) viscosity in
28 production and [16] used self-organizing map (SOM) and supervised feed-
29 forward backpropagation neural networks to estimate parameters of fermentation
30 processes with recombinant *E. coli*. However, what sets autoencoders (AEs)
31 apart is their potential to integrate predictions with the specific structural
32 characteristics of a neural network, offering unique advantages.

33 Autoencoders offer many advantages, making them an ideal choice for
34 implementing soft-sensors in various applications. Firstly, their ability to
35 perform unsupervised learning allows soft sensors to extract valuable insights
36 from unlabeled data streams, eliminating the need for costly and time-consuming
37 data annotation [17]. Secondly, autoencoders excel at dimensionality reduction,
38 enabling soft sensors to handle high-dimensional data efficiently and effectively.
39 This reduction enhances computational efficiency and simplifies data visualization
40 and interpretation [18, 19]. Thirdly, by learning compressed and robust
41 representations of the input data, autoencoders facilitate extracting relevant
42 features, making soft sensors more accurate and resilient to noise and variations
43 [17].

44 Moreover, the flexibility of autoencoders in handling different types of
45 data, such as images, time series, and text, extends soft-sensors applicability
46 to diverse industries, including manufacturing, healthcare, and finance [20].
47 In the context of industrial processes, the autoencoders capacity to handle

48 vast amounts of data is particularly appealing. In complex manufacturing
49 settings, autoencoders process a plethora of sensor data efficiently, enabling
50 real-time monitoring and control of various processes [21].

51 While autoencoders are helpful tools, optimizing neural network training
52 for autoencoder-based unsupervised learning can be challenging due to the
53 high dimensionality and complexity of the input data, the nonlinear and
54 nonconvex nature of the optimization problem, and the potential for overfitting
55 or underfitting [4]. A significant challenge of unsupervised models like autoencoders
56 is the absence of a clear, straightforward objective function to cluster data
57 points based on their semanticity [22]. Additionally, certain objective functions
58 can be overly simplistic, and when associated with the network training with
59 a high number of parameters, it can lead to issues like the optimization of
60 abnormal points and the generation of chaotic latent spaces [23]

61 To overcome these limitations, we need a way to gain more control over
62 the training and evolution of this unsupervised method aiming to limit the
63 chaos in latent spaces. The latent space can be input for constructing models
64 that predict data characteristics. In this paper, we propose novel objective
65 functions using concepts explored by Bristol [24] over multi-input, multi-
66 output problems in industrial control of gain matrix (G) and relative gain
67 array (RGA) and pruning functions using these matrices for each layer to
68 improve the training of neural networks for autoencoder-based unsupervised
69 learning. The AE's compressed latent space will be used as input for the
70 calibration of linear predictive models as soft sensors for a case study of a
71 simulation of a propene production plant [25] consisting of three distillation
72 columns and aims to distillate a load of liquefied petroleum gas.

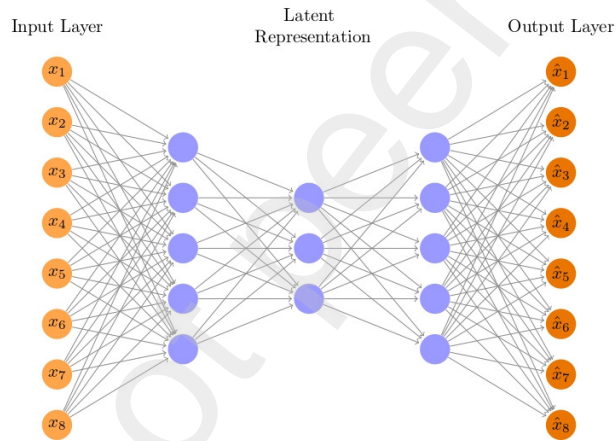
73 **2. Methodology**

74 *2.1. Autoencoder*

75 Neural networks draw inspiration from the human brains neural structure
76 [26]. It consists of interconnected nodes, called neurons, organized into layers.
77 Each neuron is an essential processing unit that receives input data and
78 performs a simple computation. It multiplies each input by a corresponding
79 weight, sums them up with a bias term, and then applies an activation
80 function to determine its output. This output is then passed on to other
81 neurons in the network. Through a process called training, neural networks
82 adjust their weights and biases to learn patterns and relationships within
83 the data, enabling them to perform tasks such as image recognition, natural

84 language processing, and decision-making with remarkable accuracy. During
85 training, neural networks utilize objective functions, also known as loss functions,
86 to measure the difference between predicted outputs and the actual targets.
87 The neural network fine-tunes its parameters by minimizing the value of the
88 objective function through optimization algorithms like gradient descent. It
89 improves its ability to make accurate predictions on unseen data [27].

90 As a class of artificial neural networks, autoencoders play a crucial role in
91 unsupervised learning and dimensionality reduction tasks [28]. The architecture
92 of an autoencoder comprises an input layer and one or more hidden layers
93 constituting the encoder and decoder segments, as illustrated in Figure 1.
94 These hidden layers generate an encoded representation of the input data,
95 subsequently reconstructed back to its original form in the output layer.



96 **Figure 1: Autoencoder Structure**

97 Autoencoders, a type of neural network, possess a captivating structure
98 where neurons interact to minimize reconstruction errors between input and
99 output during training [20]. This enables them to recreate input data from
100 encoded representations, facilitating efficient data compression and representation
101 of critical features [29]. Autoencoders find extensive applications in data
102 compression, anomaly detection, image denoising, and computer vision tasks
103 [30]. In industrial processes, they efficiently handle large datasets for real-
104 time monitoring and control [21].

105 Despite their advantages, autoencoders face challenges in generating organized
106 structures in the latent space due to non-specific objective functions and a
107 lack of good regularizations [23]

108 Nevertheless, despite these challenges, autoencoders remain powerful tools
 109 with vast potential across various applications in advancing machine learning
 110 and artificial intelligence. Ongoing research continues to address and improve
 111 upon these limitations. As this kind of model continues to be explored in
 112 various fields, there is a growing interest in developing methods of optimizing
 113 the training of these neural networks.

114 2.2. Gain Matrix (G) and Relative Gain Array(RGA)

115 To improve the training of AE models, multivariable gain matrix (G) and
 116 relative gain matrix (RGA) concepts were proposed here to formulate two
 117 modified goal functions for AE training. The first concept here introduced
 118 is the Gain matrix (G) given by:

$$G = \begin{bmatrix} \frac{\partial \hat{x}_1}{\partial x_1} & \cdots & \frac{\partial \hat{x}_1}{\partial x_n} \\ \vdots & \ddots & \vdots \\ \frac{\partial \hat{x}_m}{\partial x_1} & \cdots & \frac{\partial \hat{x}_m}{\partial x_n} \end{bmatrix} \quad (1)$$

119 where \hat{x}_m is the output m and x_n is the input n .

120 In industrial control, the gain matrix refers to a mathematical representation
 121 of the relationship between the inputs and outputs of a control system. It
 122 is commonly used in multivariable control systems with multiple inputs and
 123 outputs. Each element of the gain matrix represents the gain or sensitivity
 124 of the corresponding output to a unit change in a particular input [31].

125 The second concept is the relative gain array (RGA) proposed by Bristol
 126 (1966), which corresponds to a matrix used in multivariable control to analyze
 127 and understand the interactions between different inputs and outputs. It
 128 provides insights into the relative importance of each input to each output
 129 regarding the systems overall performance. It quantifies the impact of a
 130 change in input m on output n while holding all others. It can be calculated
 131 using (2) for a square matrix or be generalized to a $l \times m$ non-square matrix
 132 using (3).

$$RGA = G \odot (G^{-1})^T \quad (2)$$

$$RGA = G \odot (G^\dagger)^T \quad (3)$$

133 where \odot is the elementwise Hadamard product of the matrices of gain
 134 (G), and \dagger is the Moore–Penrose inverse.

135 *2.3. Objective functions and Pruning techniques*

136 *2.3.1. Objective functions*

137 Generative models, such as autoencoders, often require an objective function
138 to govern the relationship between the input data and its reconstructed
139 counterpart. The commonly employed objective function is MSE (mean
140 squared error). However, these constraints can be overly simplistic. Although
141 MSE is straightforward to solve, it tends to prioritize outliers when they exist
142 in the data. This phenomenon occurs because MSE assigns greater weight
143 to outliers, diverting the models optimization efforts towards these atypical
144 points [23]

145 The mean square error (equation 4) was used as a base equation for the
146 new objective functions.

$$MSE = \frac{1}{n} \sum_{i=1}^n (x_i - \hat{x}_i)^2 \quad (4)$$

147 where x_i is the input value of the variables and \hat{x}_i is the reconstructed
148 output n is the number of features or variables of the model.

149 The methodology of using the gain matrix and RGA as part of the
150 objective function can potentially improve the quality of unsupervised models.
151 The first objective function created uses the gain matrix (G) to incorporate
152 the interaction between each input-output into the cost function as a second
153 term, together with mean square error (equation 5).

$$f_{gain} = \frac{1}{m} \sum_{i=1}^m \left(\frac{1}{n} \sum_{i=1}^n (x_i - \hat{x}_i)^2 + \lambda (\|G - I\|_2)^2 \right) \quad (5)$$

154 where I is an identity matrix with the same dimensions as G , which is
155 obtained by the *autograd* function in PyTorch, and m is the batch size or
156 number of observations processed at a time.

157 Based on widely studied regularization functions such as Lasso (L1) and
158 Ridge (L2) described in [32], the function was developed using a lambda (λ)
159 to define the relative importance of the gain matrix, with the regularization
160 value being the norm of the matrix subtracting an identity matrix of equivalent
161 size, which has the function of correcting the value to an ideal system (no
162 interaction between the channels), plus the widely used error function MSE.

163 Likewise, for the RGA, equation 6 was developed:

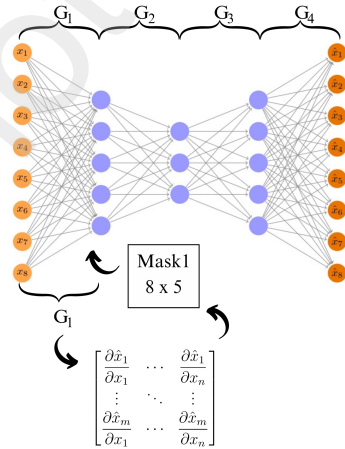
$$f_{RGA} = \frac{1}{m} \sum_{i=1}^m \left(\frac{1}{n} \sum_{i=1}^n (x_i + \hat{x}_i)^2 + \lambda (\| RGA - I \|_2)^2 \right) \quad (6)$$

164 The RGA was used in the objective function, resembling equation 5 using
 165 a lambda value (λ) and the squared Euclidean norm of the difference between
 166 RGA and an identity matrix. where I is an identity matrix with the same
 167 dimensions as RGA, and m is the batch size or number of observations
 168 processed at a time.

169 The selection of the Euclidean norm to penalize differences between matrices
 170 in an autoencoder is rooted in the objective of highlighting and amplifying
 171 noteworthy individual errors. This decision is motivated by the intention
 172 to assign greater significance to substantial deviations between the real and
 173 ideal coupling values, thereby possibly promoting a selective approach to
 174 penalization. By choosing the Euclidean norm, the attention is redirected to
 175 a more localized evaluation of errors, potentially facilitating a more precise
 176 strategy for addressing specific coupling patterns within the autoencoder
 177 architecture.

178 2.4. Pruning functions

179 For the pruning functions, gain matrices and RGAs were calculated layer
 180 by layer according to Figure 2:



181 **Figure 2:** Diagram of Gain Pruning

182 The calculated matrices were used in a pruning function that iterates
 183 over the list of weights of the layers and creates a mask that sets values lower

184 than a pre-established threshold of 0.01 to 0 throughout the training, based
185 on this and to avoid very sudden cuts, we applied these masks on the layers
186 every 25 epochs in networks that are trained for a total of 1000 epochs.

187 *2.5. Soft-Sensor methodology*

188 The soft-sensor development methodology employed in this study embraces
189 a comprehensive data-driven approach, integrating advanced process control
190 and machine learning techniques. Data preparation and analysis are conducted
191 using Python v.3.9.16, with specific libraries tailored for diverse tasks to
192 initiate the process. Pandas v.2.0.1 and NumPy v.1.21.5 are harnessed for
193 data manipulation and feature engineering. PyTorch v.2.0.0 and Scikit-learn
194 v.1.2.2 are employed to create and train predictive models. These libraries
195 leverage their capabilities for modeling and optimizing predictions based on
196 autoencoders.

197 *2.6. Data processing*

198 Given the temporal nature of the data organized in time series format, the
199 dataset was partitioned in a 60:20:20 ratio using a methodology of modified
200 systematic sampling that was guaranteed to select the samples with minimum
201 and maximum values of the output variable for the training subset, using the
202 *k*-rank method [33]. This was crucial as all samples must be within the range
203 for the black-box models so that no extrapolation would be needed [34].

204 With the split data, a normalization was applied using a Standard Scaler
205 method. This method rescaled the distribution of values, ensuring that the
206 mean of observed values was centered at 0, and the standard deviation was
207 set to 1.

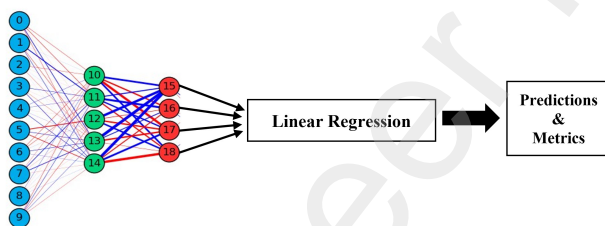
208 *2.7. Soft-sensor Structure*

209 The autoencoder hyperparameters were defined through a Grid Search of
210 hyperparameters (Table 1) to obtain the best model and capture the behavior
211 of data for each soft-sensor.

212 We aim to optimize the hyperparameters of our model effectively using
213 grid search, with a batch size fixed in 512. Our focus lies in achieving the best
214 possible settings for the autoencoder + linear model (Figure 3) by evaluating
215 its explained variance. To accomplish this, the autoencoder must first learn to
216 reconstruct the data accurately and, subsequently, utilize the encoded space
217 to make precise estimations. Through this process, we can determine the
218 optimal hyperparameters that enhance our models performance and robustness.

Table 1: Hyperparameter search space

Parameter	Search Space
Number of layers	3 or 5 layers
Activation function	Sigmoid and ReLU
Size of hidden layers	5, 6, 7 and 8 neurons
Size of latent space	4, 5, 6, 7 and 8 neurons
Learning rate	1×10^{-4} , 1×10^{-3} and 1×10^{-2}
Lambda (λ)	1, 0.1 and 1×10^{-2}



219

Figure 3: Structure of Soft-sensor

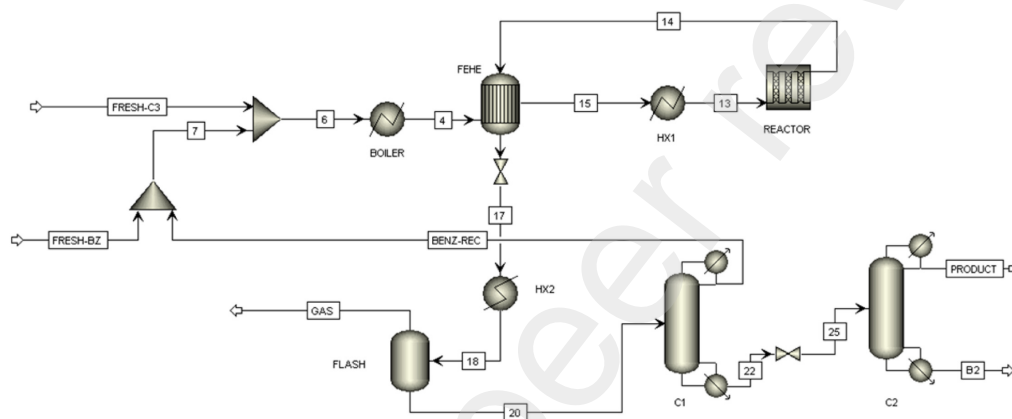
220 The grid search not only allowed us to find the best hyperparameters for
 221 our soft-sensor model but also provided valuable insights into the behavior of
 222 the autoencoder under different configurations. By systematically evaluating
 223 the models performance with various hyperparameter combinations, we better
 224 understood how each parameter impacts the models ability to reconstruct
 225 data and make accurate predictions. This knowledge proved invaluable in
 226 fine-tuning the soft sensor, ultimately leading to a highly efficient and reliable
 227 system for detecting the characteristics of our case study.

228 subsectionCase study

229 This study utilizes a simulated dataset from a propene production plant
 230 [25]. The process consists of a series of three distillation columns that will be
 231 respectively called T-01, T-02, and T-03 and is designed to separate liquefied
 232 petroleum gas into a stream containing 99.6% propene as the final product.

233 In the first column, it is important to pass on as little impurities as
 234 possible to the second column, which consists of removing the heavies (longer
 235 chain hydrocarbons). Therefore, the soft-sensor target of T-01 corresponds to
 236 the amount of impurities in the top stream. The inference of this variable is
 237 of great importance for the control of the process, since this impurity must be

238 kept to a minimum, considering the thermodynamic and economic conditions
 239 of the plant. For column T-02, the variable of most significant interest to infer
 240 is the propylene output at the top of the column, representing its waste. In T-
 241 03, it is important to control the specification of the propylene concentration
 242 at the top of the column. For this, it is necessary to infer the concentration of
 243 propane, a component that makes the propylene stream impure. An Aspen
 244 Plus® representation of the unit can be seen in Figure 4.



245 **Figure 4:** Aspen Plus® model of the unit adapted from [25]

246 Data is segregated by column, where column T-01 has 871 process operation
 247 data points with available measurements of 10 different instruments, column
 248 T-02 has 407038 entries with 11 instruments, and column T-03 has 1764 data
 249 points with 19 instruments.

250 3. Results

251 A technique called Grid Search was used to find the ideal hyperparameters
 252 for the neural networks used in this study. Grid Search is a thorough search
 253 method that allows exploring various possible combinations of hyperparameters
 254 to determine the optimal configuration of the model. In Table 2, presented
 255 below, the best hyperparameters for each column are presented as obtained
 256 in the optimization.

257
 258 After adjusting the autoencoders using the optimized hyperparameters,
 259 they were used in soft-sensors with linear regression to detect the characteristics
 260 addressed in the case study. The adjusted autoencoders made it possible to

Table 2: Selected hyperparameters

Hyperparameter	Columns		
	T-01	T-02	T-03
Layers	5	5	5
Hidden Neurons	5	7	10
Encoded size	4	3	4
Activation	Sigmoid	Sigmoid	Sigmoid
Learning rate	1×10^{-2}	1×10^{-2}	0.1
Lambda	0.1	0.1	1×10^{-2}

261 compress the original data information into lower-dimensional representations,
262 preserving the most relevant characteristics. To evaluate the performance
263 of the adjusted autoencoders, Table 3 was generated, which present the
264 explained variances by the different models in comparison. The results of
265 the models developed in this study were compared with a PCA (Principal
266 Component Analysis) and a conventional autoencoder that uses the same
267 configuration with an MSE objective function.

268 After analyzing the results presented in Table 3, we further validated
269 the significance of the differences between the soft-sensor models using the
270 Fisher Least Significant Difference (LSD) method. The Fisher LSD method
271 is a statistical test commonly employed in multiple comparisons to determine
272 if there are significant differences between the means of different groups. Our
273 study applied it to verify the differences in explained variances obtained by
274 the various soft-sensor models across columns T-01, T-02, and T-03.

275 The Fisher LSD test revealed statistically significant differences ($p < 0.05$)
276 between several pairs of soft-sensor models, providing additional evidence
277 that the proposed novel objective functions, which integrate the gain matrix
278 and relative gain array, substantially impact the models performance.

279 Comparing the results, it is observed that the autoencoders with novel
280 functions obtained a higher explained variance concerning the reference methods.
281 This indicates that the soft sensors developed in this study could capture the
282 relevant information in the input data more accurately. Works by authors
283 such as [35, 36, 37] show that autoencoders, in many applications, tend
284 to outperform linear methods such as PCA, being able to detect subtle
285 anomalies in data. This more remarkable ability to explain variances indicates

Table 3: Explained variance for each soft sensor in columns T-01, T-02 and T-03.

Model	Columns		
	T-01	T-02	T-03
PCA	0.66 ± 0.0^a	0.03 ± 0.0^{ab}	0.46 ± 0.0^a
AE	0.82 ± 0.0^{bc}	0.34 ± 0.21^{cd}	0.65 ± 0.02^{bc}
GAE	0.89 ± 0.08^{bc}	0.55 ± 0.04^{de}	0.64 ± 0.09^{bc}
RGAE	0.79 ± 0.02^{ab}	0.33 ± 0.18^{cd}	0.57 ± 0.08^{ab}
AE PG	0.79 ± 0.07^{ab}	0.59 ± 0.02^e	0.79 ± 0.07^{cd}
AE PRGA	0.90 ± 0.06^{bc}	0.02 ± 0.0^a	0.59 ± 0.04^{ab}
GAE PG	0.81 ± 0.03^{bc}	0.46 ± 0.14^{cde}	0.67 ± 0.08^{bc}
GAE PRGA	0.81 ± 0.12^{bc}	0.26 ± 0.04^{bc}	0.63 ± 0.14^b
RGAE PG	0.86 ± 0.07^{bc}	0.46 ± 0.14^{cde}	0.88 ± 0.04^d
RGAE PRGA	0.93 ± 0.04^c	0.32 ± 0.01^c	0.63 ± 0.08^b

^a first group; ^b second group; ^c third group; ^d fourth group; ^e fifth group in Fisher's Test.

286 that the adjusted autoencoders perform better in the data compression and
 287 reconstruction task than the PCA and the conventional autoencoder.

288 Moreover, by observing the behavior of the network weights during training
 289 and at the end of it (Figure 5) we can verify simpler relationships between
 290 neurons, showing a potential to reduce the interaction between channels and
 291 consequently reduce the number of variables adjusted to each training epoch.

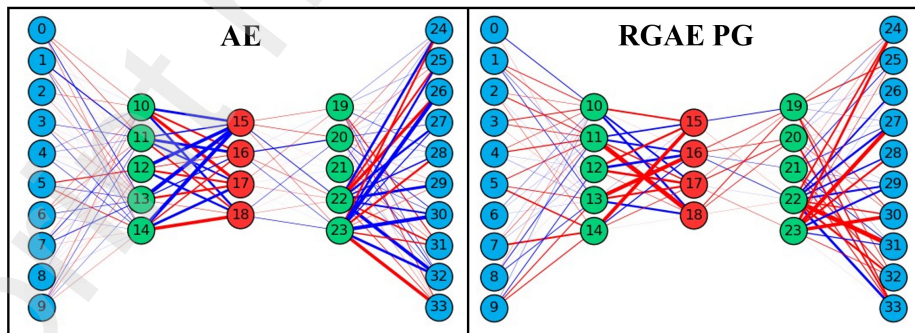


Figure 5: Visual comparison of T-01 column weights for a normal autoencoder (AE) and an autoencoder that uses the functions developed in the article (RGAE PG) after training

293 These results reinforce the importance of the specific functions developed
294 in this work to adjust the autoencoders more appropriately to the problem in
295 question, thus improving the quality of the latent representations obtained
296 and, consequently, the ability to explain data variances.

297 **4. Conclusions**

298 In conclusion, this study demonstrates the effectiveness of autoencoders
299 in addressing the challenges of high-dimensional data analysis. By leveraging
300 the latent space representation generated by autoencoders, valuable insights
301 can be extracted from complex datasets, leading to improved predictions and
302 data-driven decision-making. Incorporating novel objective functions based
303 on Gain Matrix (G) and Relative Gain Array (RGA) concepts, along with
304 pruning techniques, enhances the training and performance of autoencoder
305 models.

306 The case study results, focused on a simulated propene production plant,
307 highlight the superiority of autoencoders with novel objective functions compared
308 to traditional methods such as PCA and conventional autoencoders with
309 the aim of MSE functions. These autoencoders achieve higher explained
310 variance and accurately capture the relevant information in the input data,
311 surpassing linear methods and enabling the detection of subtle anomalies.
312 The observed behavior of network weights during training further indicates a
313 potential reduction in channel interactions, enhancing the models efficiency
314 and simplifying relationships between neurons.

315 Overall, this research underscores the potential of autoencoders as powerful
316 tools for high-dimensional data analysis and soft-sensors. By refining the
317 objective functions and incorporating multivariable control concepts, autoencoders
318 can provide better control over the training process and improve the quality of
319 latent representations. Future work may explore diverse datasets and extend
320 the application of autoencoders to various real-world scenarios, offering new
321 opportunities for addressing complex data challenges and advancing the field
322 of data science.

323 **5. Declaration of Generative AI and AI-assisted technologies in the** 324 **writing process**

325 During the preparation of this work the author(s) used ChatGPT in order
326 to improve readability. After using this tool/service, the author(s) reviewed

327 and edited the content as needed and take(s) full responsibility for the content
328 of the publication.

329 **References**

- 330 [1] M. Verleysen, D. François, The curse of dimensionality in data mining
331 and time series prediction, in: J. Cabestany, A. Prieto, F. Sandoval
332 (Eds.), *Computational Intelligence and Bioinspired Systems*, Springer
333 Berlin Heidelberg, Berlin, Heidelberg, 2005, pp. 758–770.
- 334 [2] W. Wang, Y. Huang, Y. Wang, L. Wang, Generalized autoencoder: A
335 neural network framework for dimensionality reduction, *IEEE Computer
336 Society Conference on Computer Vision and Pattern Recognition
337 Workshops* (2014) 496–503doi:10.1109/CVPRW.2014.79.
- 338 [3] D. Charte, F. Charte, S. Garcia, M. J. del Jesus, F. Herrera, A practical
339 tutorial on autoencoders for nonlinear feature fusion: Taxonomy,
340 models, software and guidelines, *Information Fusion* 44 (2018) 78–96.
341 doi:10.1016/J.INFFUS.2017.12.007.
- 342 [4] D. Bank, N. Koenigstein, R. Giryes, Autoencoders, *arXiv e-prints* 2
343 (2020). doi:10.48550/arXiv.2003.05991.
- 344 [5] X. Wu, Q. Cheng, Fractal autoencoders for feature selection, *35th AAAI
345 Conference on Artificial Intelligence, AAAI 2021 12A* (2020) 10370–
346 10378. doi:10.48550/arxiv.2010.09430.
- 347 [6] R. Clarke, H. W. Resson, A. Wang, J. Xuan, M. C. Liu, E. A. Gehan,
348 Y. Wang, The properties of high-dimensional data spaces: implications
349 for exploring gene and protein expression data, *Nature Reviews Cancer*
350 2008 8 (2008) 37–49. doi:10.1038/nrc2294.
- 351 [7] G. E. Hinton, R. R. Salakhutdinov, Reducing the dimensionality
352 of data with neural networks, *Science* 313 (2006) 504–507.
353 doi:10.1126/science.1127647.
- 354 [8] J. Deng, Z. Zhang, F. Eyben, B. Schuller, Autoencoder-
355 based unsupervised domain adaptation for speech emotion
356 recognition, *IEEE Signal Processing Letters* 21 (2014) 1068–1072.
357 doi:10.1109/LSP.2014.2324759.

- 358 [9] I. P. Yamshchikov, A. Tikhonov, Music generation with variational
359 recurrent autoencoder supported by history, SN Applied Sciences 2
360 (2017). doi:10.1007/s42452-020-03715-w.
- 361 [10] C. Doersch, Tutorial on variational autoencoders, ArXiv e-prints
362 stat.ML (2016). doi:10.48550/arXiv.1606.05908.
- 363 [11] J. Almotiri, K. Elleithy, A. Elleithy, Comparison of autoencoder
364 and principal component analysis followed by neural network
365 for e-learning using handwritten recognition, 2017 IEEE Long
366 Island Systems, Applications and Technology Conference (2017).
367 doi:10.1109/LISAT.2017.8001963.
- 368 [12] C. Shang, F. Yang, D. Huang, W. Lyu, Data-driven soft sensor
369 development based on deep learning technique, Journal of Process
370 Control 24 (2014) 223–233. doi:10.1016/J.JPROCONT.2014.01.012.
- 371 [13] X. Yuan, Y. Wang, C. Yang, W. Gui, Stacked isomorphic autoencoder
372 based soft analyzer and its application to sulfur recovery unit,
373 Information Sciences 534 (2020) 72–84. doi:10.1016/J.INS.2020.03.018.
- 374 [14] G. Civelekoglu, A. Perendeci, N. O. Yigit, M. Kitis, Modeling carbon
375 and nitrogen removal in an industrial wastewater treatment plant using
376 an adaptive network-based fuzzy inference system, CLEAN - Soil, Air,
377 Water 35 (2007) 617–625. doi:10.1002/CLEN.200700076.
- 378 [15] J. Gonzaga, L. Meleiro, C. Kiang, R. M. Filho, Ann-based soft-
379 sensor for real-time process monitoring and control of an industrial
380 polymerization process, Computers & Chemical Engineering 33 (2009)
381 43–49. doi:10.1016/j.compchemeng.2008.05.019.
- 382 [16] K.-I. Lee, Y.-S. Yim, S.-W. Chung, J. Wei, J. I. Rhee, Application
383 of artificial neural networks to the analysis of two-dimensional
384 fluorescence spectra in recombinant e coli fermentation processes,
385 Journal of Chemical Technology & Biotechnology 80 (2005) 1036–1045.
386 doi:10.1002/JCTB.1281.
- 387 [17] S. M. Miraftebzadeh, M. Longo, M. Brenna, Knowledge
388 extraction from pv power generation with deep learning
389 autoencoder and clustering-based algorithms, IEEE Access (2023).
390 doi:10.1109/ACCESS.2023.3292516.

- 391 [18] O. Kuchaiev, B. Ginsburg, Training deep autoencoders for collaborative
392 filtering, *ArXiv e-prints* 3 (2017). doi:10.48550/arXiv.1708.01715.
- 393 [19] J. Bharadiya, J. P. Bharadiya, A tutorial on principal component
394 analysis for dimensionality reduction in machine learning, Article in
395 *International Journal of Innovative Research in Science Engineering and
396 Technology* 8 (2023). doi:10.5281/zenodo.8002436.
- 397 [20] S. Chen, W. Guo, Auto-encoders in deep learning - a
398 review with new perspectives, *Mathematics* 11 (2023) 1777.
399 doi:10.3390/MATH11081777.
- 400 [21] A. L. Alfeo, M. G. Cimino, G. Manco, E. Ritacco, G. Vaglini,
401 Using an autoencoder in the design of an anomaly detector for
402 smart manufacturing, *Pattern Recognition Letters* 136 (2020) 272–278.
403 doi:10.1016/J.PATREC.2020.06.008.
- 404 [22] N. Mrabah, N. M. Khan, R. Ksantini, Deep clustering with a dynamic
405 autoencoder smart vision view project landmine detection view project
406 deep clustering with a dynamic autoencoder, *ArXiv e-prints* 5 (2019).
407 doi:10.48550/arXiv.1901.07752.
- 408 [23] Q. Zhu, H. Wang, R. Zhang, Wavelet loss function for auto-encoder,
409 *IEEE Access* 9 (2021) 27101–27108. doi:10.1109/ACCESS.2021.3058604.
- 410 [24] E. H. Bristol, On a new measure of interaction for multivariable
411 process control, *IEEE Transactions on Automatic Control* (1966).
412 doi:10.1109/TAC.1966.1098266.
- 413 [25] E. S. Schultz, J. O. Trierweiler, M. Farenzena, The importance
414 of nominal operating point selection in self-optimizing control,
415 *Industrial and Engineering Chemistry Research* 55 (2016) 7381–7393.
416 doi:10.1021/acs.iecr.5b02044.
- 417 [26] R. B. Gharbi, G. A. Mansoori, An introduction to artificial
418 intelligence applications in petroleum exploration and production,
419 *Journal of Petroleum Science and Engineering* 49 (2005) 93–96.
420 doi:10.1016/J.PETROL.2005.09.001.

- 421 [27] J. Zou, Y. Han, S. S. So, Overview of Artificial Neural Networks,
422 Humana Press, Totowa, NJ, 2009, pp. 14–22. doi:10.1007/978-1-60327-
423 101-1_2.
- 424 [28] M. Sewak, S. K. Sahay, H. Rathore, An overview of deep learning
425 architecture of deep neural networks and autoencoders, Journal
426 of Computational and Theoretical Nanoscience 17 (2020) 182–188.
427 doi:10.1166/JCTN.2020.8648.
- 428 [29] E. Trunz, M. Weinmann, S. Merzbach, R. Klein, Efficient
429 structuring of the latent space for controllable data reconstruction
430 and compression, Graphics and Visual Computing 7 (2022) 200059.
431 doi:10.1016/J.GVC.2022.200059.
- 432 [30] P. Li, Y. Pei, J. Li, A comprehensive survey on design and application
433 of autoencoder in deep learning, Applied Soft Computing 138 (2023)
434 110176. doi:10.1016/J.ASOC.2023.110176.
- 435 [31] S. Skogestad, I. Postlethwaite, Multivariable Feedback Control Second
436 Edition: Analysis and Design, n.2 Edition, Wiley & Sons, Incorporated,
437 John, 2005.
- 438 [32] L. E. Melkumova, S. Y. Shatskikh, Comparing ridge and lasso
439 estimators for data analysis, Procedia Engineering 201 (2017) 746–755.
440 doi:10.1016/J.PROENG.2017.09.615.
- 441 [33] P. V. Santos, L. Ranzan, M. Farenzena, J. O. Trierweiler, K-rank:
442 An evolution of y-rank for multiple solutions problem, Brazilian
443 Journal of Chemical Engineering 36 (2019) 409–419. doi:10.1590/0104-
444 6632.20190361S20170455.
- 445 [34] P. Kadlec, B. Gabrys, S. Strandt, Data-driven soft sensors in the
446 process industry, Computers & Chemical Engineering 33 (2009) 795–
447 814. doi:10.1016/J.COMPCHEMENG.2008.12.012.
- 448 [35] M. A. Helal, S. Eldawlatly, M. Taher, Using autoencoders for feature
449 enhancement in motor imagery brain-computer interfaces, 2017 13th
450 IASTED International Conference on Biomedical Engineering (BioMed)
451 (2017) 89–93doi:10.2316/P.2017.852-052.

- 452 [36] A. M. Tăutan, A. C. Rossi, R. D. Francisco, B. Ionescu, Dimensionality
453 reduction for eeg-based sleep stage detection: comparison of
454 autoencoders, principal component analysis and factor analysis,
455 Biomedical Engineering / Biomedizinische Technik 66 (2020) 125–136.
456 doi:10.1515/BMT-2020-0139.
- 457 [37] P. Korkos, J. Kleemola, M. Linjama, A. Lehtovaara, Representation
458 learning for detecting the faults in a wind turbine hydraulic pitch system
459 using deep learning, Energies 15 (2022). doi:10.3390/EN15249279.